Full Paper: A new method for the analysis of small-angle X-ray scattering (SAXS) of anisotropic samples is introduced in the field of thermoplastic elastomers. It results in a detailed picture of the complex two-phase nanostructure and its range of order as a function of strain. A linear triblock copolymer from polystyrene and polyisoprene (SIS) and a brominated sample are studied as a function of elongation by ultra-small-angle X-ray scattering (USAXS) from synchrotron. The styrene content is 30%. Two-dimensional scattering patterns are transformed to the Laplacian of the two-dimensional correlation function. Analysis of this chord distribution function (CDF) is demonstrated and compared to direct analysis of the fiber patterns. CDF analysis proves to be superior, especially when the description of lateral arrangement of domains is concerned. Neat isotropic SIS reveals remarkable long-range order. When strained to high elongation, it exhibits elongated cylindrical domains arranged in a macro-lattice, whereas the brominated material shows almost spherical domains arranged in microfibrils with some lateral order. Domain shape and arrangement is determined.

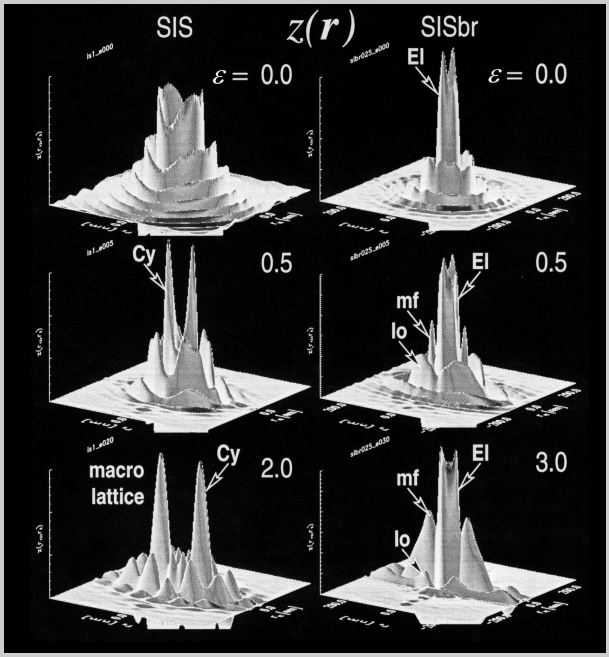

Three-dimensional top view ("*domain face*") $z(\mathbf{r})$ of the CDF as a function of elongation for neat (SIS) and brominated (SISbr) triblock copolymer. "El" marks peaks from an ellipsoidal particle. "Cy" points at cylinder peaks. "mf" indicates microfibril peaks on the meridian and "lo" shows lateral order by domain-domain correlations.

Nanostructure Evolution of SIS Thermoplastic Elastomers During Straining as Revealed by USAXS and Two-Dimensional Chord Distribution Analysis

*Norbert Stribeck,**[1] *Emil Buzdugan,*[2a] *Paul Ghioca,*[2] *Sever Şerban,*[2] *Rainer Gehrke*[3]

[1] Institut f. Technische u. Makromolekulare Chemie, Universität Hamburg, Bundesstr. 45, 20146 Hamburg, Germany
Fax: +49 40 42838 6008; E-Mail: Norbert.Stribeck@desy.de
[2] Chemical Research Institute ICECHIM, Spl. Independentei 202, 77208 Bucharest, Romania
Fax: +40 1 312 3493; E-Mail: ebuzdugan@chimfiz.icf.ro
[3] HASYLAB at DESY, Notkestr. 85, 22603 Hamburg, Germany
Fax: +49 40 8998 2787; E-Mail: Rainer.Gehrke@desy.de

Keywords: block copolymers; microstructure; multidimensional; SAXS; strain

1 Introduction

The determination of structural parameters from small-angle scattering patterns has been a problem of constant interest for many years, especially in the field of synthetic polymer materials, many of which can be considered two-phase systems. The basic properties of scattering-from a two-phase system have been discussed by Porod.[1] Debye's general correlation function[2] has paved the way for analysis of scattering data from distorted structures in the physical space. The practical applicability of this concept for the case of a lamellar two-phase system has been exhausted in Vonk's papers on the one-dimensional correlation function.[3–5] Moreover, Vonk proposed a gener-

[a] Present address: Center for Biotechnology and Bioengineering, University of Pittsburgh, Pittsburgh PA 15219, USA
Fax: +1 412 383 9710; E-Mail: buzdugan@engrng.pitt.edu

  1022-1352/2002/0403–0636$17.50+.50/0

alization of this method to the two-dimensional case[6] and applied it to a study of polyethylene fibers. Employing the concept of correlation function, the considerable influence of polydispersity on scattering data can unfortunately only be taken into account in a rudimentary way. Thus correlation function analysis, in virtually any practical case, assumes that layer thicknesses in the lamellar system vary little about an average value.[7] Consequences of this simplification are documented.[8] Resort to this dilemma has been devised by Tchoubar and Méring.[9–13] Their chord distribution function (CDF) is the second derivative of the isotropic general correlation function and it is built from particle size distributions, which are considered basic to structural analysis. This concept became applicable for a wide range of practical problems by the interface distribution function (IDF), as deduced by Ruland.[14–16] For isotropic lamellar two-phase systems or perfectly oriented microfibrillar systems, the interface distribution analysis permits the extraction of maximal structural information from SAXS and is gaining more and more favor.[17] Even for cases in which an orientation distribution is to be considered, a solution has been indicated.[18–20]

Continuing in this direction, a semi-automatic method for the computation of a multi-dimensional chord distribution from small-angle X-ray scattering (SAXS) patterns has recently been proposed.[21] Here it shall be demonstrated, how this method can be utilized to proceed aiming at complete quantitative analysis of anisotropic data from SAXS in the field of strained thermoplastic elastomers. For many of these materials ordered bicontinuous phases have been found,[22, 23] which are best identified by SAXS,[24] and have some impact on materials properties. It is expected that the proposed method may help to elucidate the transformation from a long-range-ordered bicontinuous phase to a short-range-ordered nanostructure frequently observed in the strained state.

By bromination of styrene–diene block copolymers useful intermediate materials for subsequent chemical reactions, such as grafting or substitution reactions, are obtained.[25] As reported in a previous study, mechanical properties vary significantly as a function of bromination level.[26] Already at low bromination levels (2.5% to 7.5%), a considerable decrease of yield strength was observed and explained by a reduction of bridges among polystyrene domains. In addition, elasticity increased for low levels of bromination. Now an advanced analysis of the underlying nanostructural features from small-angle scattering data shall be demonstrated.

2 Experimental Part

Material

Commercial SIS triblock copolymer CAROM TLI 30 (CAROM S.A., Oneşti, Romania) with a total molecular mass of $\overline{M}_w = 105\ kg \cdot mol^{-1}$ was investigated. Molecular mass of the polyisoprene middle block is $\overline{M}_w = 73.5\ kg \cdot mol^{-1}$. According to IR spectroscopy the polyisoprene block contains 88.9% 1,4–*cis* units, 2.1% 1,4–*trans* units and 9.0% 3,4(*vinyl*) units. Neat material (sample designation: SIS) and a brominated sample (designation: SISbr) were studied.

Bromination and Sample Preparation

As described elsewhere[25] bromination was carried out in tetrahyrofuran (THF) solution at 0 °C. The brominated block copolymer was characterized by elemental analysis and IR spectroscopy. The bromine content of sample SISbr is 2.5% with respect to the isoprene. At this low level of bromination the bromine reacts mainly with the (1,4)-type double bonds.[25] Films of approx. 400-μm thickness were obtained by spin–casting directly from the THF solution used for the bromination.[26, 27]

Scattering Experiments

Ultra-small-angle X-ray scattering (USAXS) was performed in the synchrotron beam line BW4 at HASYLAB, Hamburg, Germany. The wavelength of the X-ray beam was 0.1381 nm. USAXS images were collected by a two-dimensional position-sensitive Gabriel detector (512×512 pixels of $0.4 \times 0.4\ mm^2$) (from European Molecular Biological Laboratory, EMBL). The sample-to-detector distance was set to 12870 mm. The minimal accessible scattering angle corresponded to a *d*-spacing of 900 nm. The maximal scattering angle corresponded to 19 nm. Samples with marks were mounted in a straining stage positioned in the synchrotron beam, slowly strained up to the desired elongation and exposed for 30 min. Images were corrected for flat-detector response and blind areas were masked. Background subtraction and sample absorption were subsequently applied. The center and fiber axis of the pattern were determined. Images were aligned and averaged with respect to the four quadrants resulting in peak maximum counts of at least 10000 (Sample SIS at highest elongation).

To cover a wider angular range, SAXS measurements were carried out at HASYLAB, beamline A2, using image plate exposed for 60 s. Here the maximal scattering angle corresponded to 4 nm.

3 CDF Analysis

The Chord Distribution $z(\mathbf{r})$

Evaluation of the scattering patterns was accomplished by a recently proposed method[21] employing a multi-dimensional chord distribution function (CDF) $z(\mathbf{r})$, which is proportional to the Laplacian $\Delta\gamma(\mathbf{r})$ of the correlation function $\gamma(\mathbf{r})$. $z(\mathbf{r})$ exhibits the correlations among the surfaces of domains in a multi-phase system in two or three dimensions with respect to physical space vector $\mathbf{r}$. More precisely it is the autocorrelation of the gradient vector field $\nabla\rho(\mathbf{r})$ of the electron density $\rho(\mathbf{r})$. For a multi-phase system $\nabla\rho(\mathbf{r})$ vanishes almost everywhere except at domain surfaces.

In the special case of fiber symmetry considered in this study $z(\mathbf{r}) = (r_{12}, r_3)$ is two-dimensional and describes the correlations among domain surfaces in (r_{12}, r_3)-plane with r_{12} indicating the equatorial and r_3 the meridional direction. Here it is proportional to the Laplacian of Vonk's two-dimensional correlation function[6, 28] $\gamma_2(\mathbf{r})$.

Computation

$z(\mathbf{r}) = (r_{12}, r_3)$ is computed from the scattering intensity $I(\mathbf{s}) = (s_{12}, s_3)$. The modulus of the scattering vector, $s = \sqrt{s_{12}^2 + s_3^2}$, is defined by $s = (2/\lambda) \sin\theta$ with the scattering angle 2θ and the wavelength of radiation λ. s_{12} and s_3 denominate the equatorial and the meridional direction in reciprocal space, respectively. Computation comprises several steps.[21] (I) A projection of the scattering intensity from reciprocal space onto the fiber plane. (II) A multiplication by $-4\pi^2 s^2$ representing the physical-space Laplacian in reciprocal space. (III) Computation of a two-dimensional background by low-pass spatial frequency filtering of the image. (IV) Subtraction of the background. (V) Two-dimensional Fourier transformation.

Intensity Background

Part of the method is a proposed solution for the problem of background subtraction in the field of SAXS. It rests on the notion that SAXS data represents spatial frequency information on nanostructure and that the information on nanostructure morphology is embedded between low-frequency background and high-frequency noise.

Interpretation

In the case of fiber symmetry $z(\mathbf{r})$ can be depicted by a surface in space which shows positive and negative peaks with respect to the (r_{12}, r_3)-plane. It can be interpreted employing Porod's "particle–ghost" notion[28–31] after minor modification (Figure 1).

Whereas the value of the correlation function $\gamma(\mathbf{r})$ as a function of ghost displacement $\mathbf{r}'$ is determined by the volume shared by particle and ghost; the value of the chord distribution $z(\mathbf{r})$ is given by the scalar product of the gradient vectors. Obviously there are only contributions at those positions where the surfaces of particle and ghost are shared. Obviously the value of $z(\mathbf{r})$ is not only a function of the number of interacting surface elements, but also a function of their orientation. Surfaces crossing at right angles do not contribute. Parallel and antiparallel gradient vectors generate function values of different sign. The sign of $z(\mathbf{r})$ is chosen to let autocorrelation of antiparallel gradient vectors generate a positive contribution to $z(\mathbf{r})$. For example, the highlighted pair of gradient vectors in the figure will contribute almost the maximal positive value. It is obvious that ghost-displacement in an ensemble of particles with convex shape will not start to generate negative contributions to $z(\mathbf{r})$ before ghosts start to overlay alien particles. Thus the corresponding negative contributions can be considered a generalization of translational repeat, whereas positive contributions are related to domain (and intermitted domain) sizes. The former are generalizations of a lattice property, whereas the latter are related to the domain shapes and distributions of multi-phase structure. Considering limiting cases, a chord distribution with positive values only describes an ensemble of uncorrelated domains. On the other hand, pronounced and repeated negative peaks indicate (lattice-like) correlations among domains.

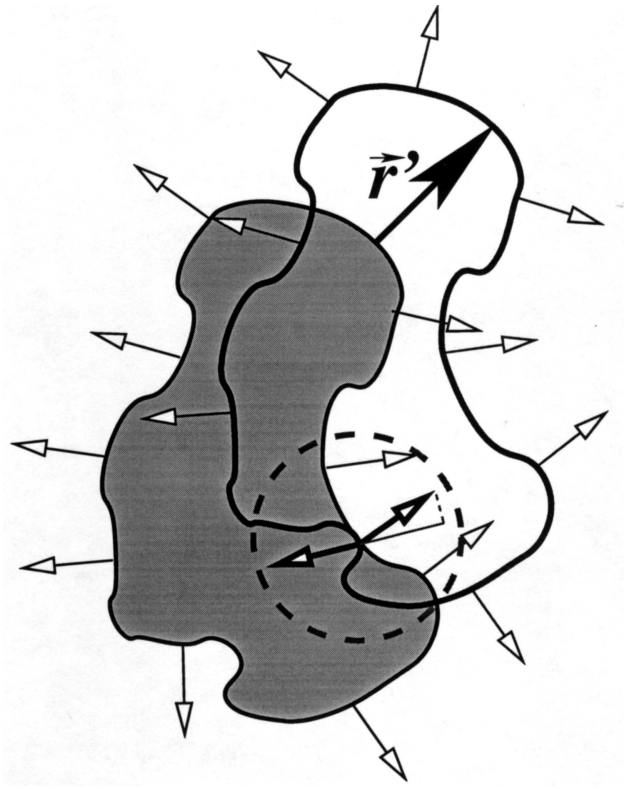

Figure 1. Particle-ghost autocorrelation of gradient vectors generates the multi-dimensional chord distribution. Its positive and negative values are a function of relative surface orientation.

When a chord distribution surface is inspected, the characteristics of the *domain face peaks* should be compared to the characteristics of the *lattice face peaks*. In this manner, fundamental insight concerning domain shape and arrangement in the nanocomposite can be achieved.

4 Results

Figure 2 shows selected contour plots of the two-dimensional USAXS patterns from the unbrominated (left) and the brominated (right) SIS triblock copolymer as a function of elongation $\varepsilon = (\ell - \ell_0)/\ell_0$ (from top to bottom).

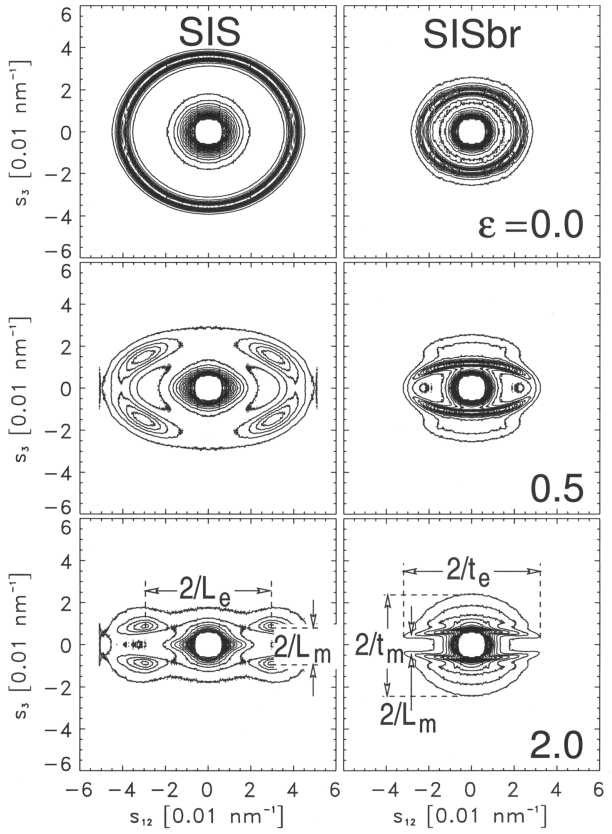

Figure 2. USAXS patterns of pure (SIS) and brominated (SISbr) poly(styrene-*block*-isoprene-*block*-styrene) copolymer as a function of elongation. Determination of structural parameters by direct analysis is indicated in the botton patterns. Meridional direction is vertical.

Direct Analysis

Following conventional analysis, scattering patterns are interpreted based on fundamental notions on structure–scattering relationship. The patterns at $\varepsilon = 0$, for instance, are almost isotropic. Slight deviation is caused from sample preparation by spin casting. The reflection ring of the brominated sample is narrower than the corresponding one of the neat SIS. From the maximum positions in the equatorial direction, long periods of 25 nm for SIS and 44 nm for SISbr are computed.

In particular for SIS block copolymers, bicontinuous phases with long-ranging order based on cubic macro-lattices have been reported. In the scattering pattern of the isotropic sample such a phase is detected from sharp Bragg reflections. We have tested numerous block copolymer samples using SAXS at larger scattering angles and have seen the bicontinuous gyroid structure. But with the samples presented here a bicontinuous structure was not detected.

Starting from $\varepsilon = 0.5$ the elastomers exhibit anisotropy. In the figures, fiber axis s_3 (meridian) is in vertical direction. With SIS, the intensity splits into four discrete reflections; with SISbr a bent layer line is observed. Both structures are not perfectly oriented, causing additional ambiguity in interpretation. In the left pattern one would have to choose between a distorted macro-lattice[32] of cylinders, and a system of tilted lamellae. Concerning the right pattern, one would rest interpretation upon either a system of uncorrelated microfibrils, or on lamellar structures with a peculiar orientation distribution.

Based on the bottom images at $\varepsilon = 2.0$, the notions mentioned first appear to be more reasonable. At nearly perfect orientation SIS proves to be a distorted macro-lattice. $L_e \approx 30$ nm indicates the lattice constant in equatorial direction. $L_m \approx 110$ nm is the lattice constant in the fiber direction. The pronounced anisotropy of the outer contour line (envelope) exhibits that the scattering domains are thin and elongated cylinders. With the SISbr sample on the right, now almost flat layer-line reflections are observed. Here the envelope is almost circular. Thus the particles are almost spherical. From the reciprocal length of the layer lines we obtain a value for the thickness of the ellipsoids (t_e) of ca. 30 nm. The aspect ratio is computed from $t_m/t_e \approx 4/3$. The distance between the layer lines (L_m) results in a long period ≈130 nm, if computed from the distance at the center of the slightly bent layer line, or of ≈190 nm, if it is computed from the distance between the ends.

Complexity of the Nanostructure

Contour plots reproduce only part of the information contained inthe USAXS pattern. The elevated data quality from modern synchrotron radiation sources requires adapted visualization. Examining three-dimensional plots of the scattering intensity (Figure 3), it becomes obvious that the complex shape of the scattering pattern cannot be explained in terms of the common simple notions on polymer nanostructure.

Nanostructure Representation in Physical Space

Contour plots of the two-dimensional chord distribution function $z(\mathbf{r})$ (Figure 4) present a visualization of the nanostructure in physical space.

At zero elongation, SIS shows many pronounced correlations among domainson a macro-lattice with a long period of $L_e = 27$ nm. SISbr, on the other hand, exhibits a fast decay of the correlations on a lattice with a long period of $L_e = 47$ nm. Comparison shows that long periods determined both from the scattering pattern and the CDF by a simple graphical method are close. As a function of increasing elongation, the central domain expands in meridional direction and a pronounced central "watch-shaped" region is formed for both samples. This region contains the information on the autocorrelation of both the polystyrene domains and the polyisoprene matrix material. It is surrounded by peaks describing the correla-

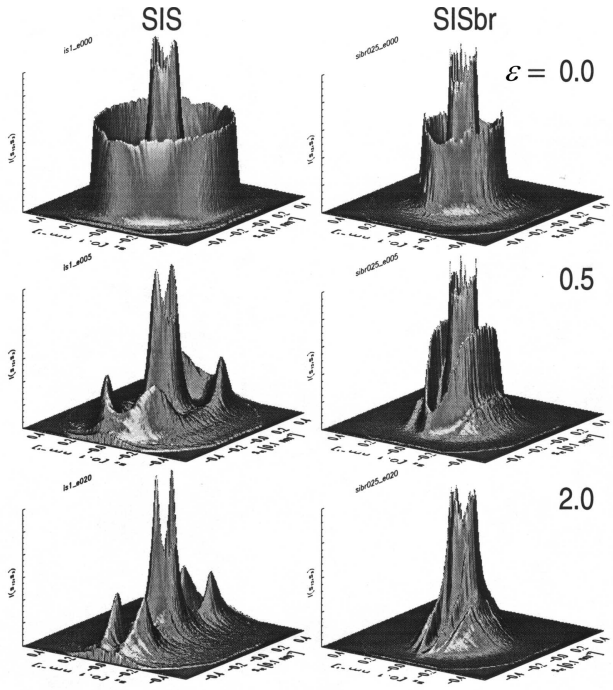

Figure 3. USAXS intensity as a function of elongation for neat (SIS) and brominated (SISbr) triblock copolymer.

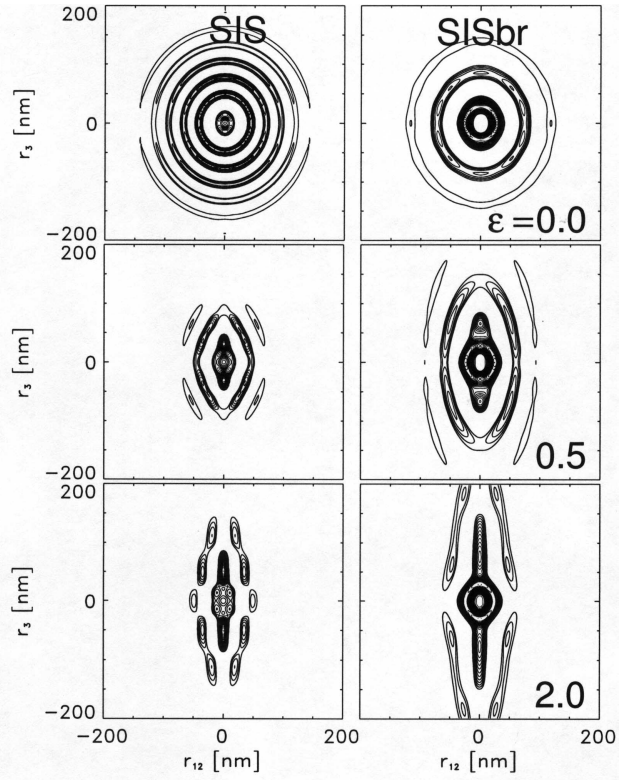

Figure 4. Contour plots of the positive peaks in the chord distribution $z(\mathbf{r})$ as a function of elongation for neat (SIS) and brominated (SISbr) triblock copolymer.

tion among different domains. In between, deep "long-period valleys" extend in meridional direction. The SIS sample, in particular, shows a very high degree of order which shall be discussed in the following section.

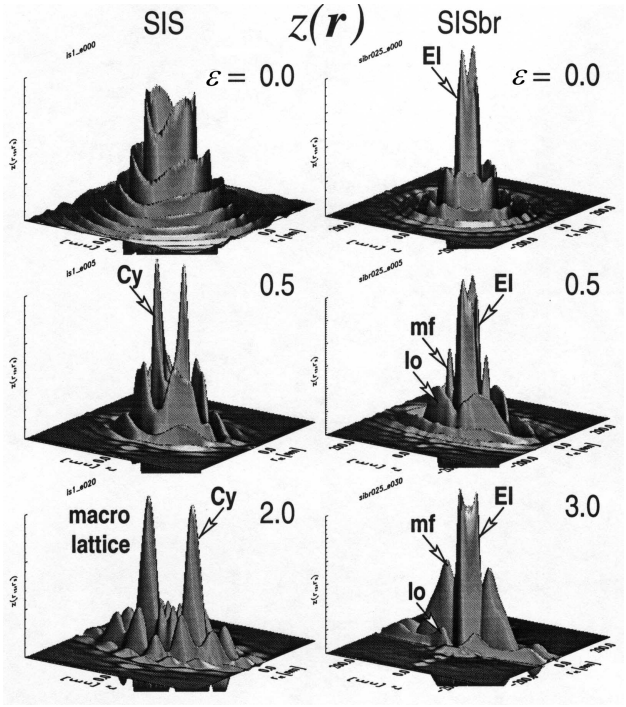

Figure 5. Three-dimensional top view ("*domain face*") $z(\mathbf{r})$ of the CDF as a function of elongation for neat (SIS) and brominated (SISbr) triblock copolymer. "El" marks peaks from an ellipsoidal particle. "Cy" points at cylinder peaks. "mf" indicates microfibril peaks on the meridian and "lo" shows lateral order by domain-domain correlations.

But before the contours at high elongation will be used to extract some quantitative information, the general nanostructural model shall be distinguished from three-dimensions plots of the chord distribution presented in Figure 5 and Figure 6 (Patterns from $\varepsilon = 3$ were chosen for sample SISbr, because the observable features become somewhat more distinct at higher elongation). Based on the "particle-ghost-displacement" notion the peaks from the CDF can be attributed to nanostructural features. In the three-dimensions representations of Figure 5 characteristic peaks are labeled. A cylinder ("Cy") gives strong peaks whenever the flat caps of particle and ghost touch at the meridian. An ellipsoid ("El") gives a strong ring close to the center. Increased intensity of this ring at the meridian can be explained by flattened caps of the ellipsoidal particles. A microfibrillar ("mf") nanostructure is revealed by a pair of additional strong peaks on the meridian. Its maxima are found at the most probable length of the elastic gap between two polystyrene domains. An outward shoulder reveals the dimension of a composite particle made from two neighboring polystyrene ellipsoids with one gap length in between. Such structure is not observed in the CDF from sample SIS. Instead, four small peaks surrounding the center indicate the shortest correlated displacement between neighboring cylinder caps in a macro-lattice.

Figure 6 is a bottom view of the CDF. It reveals the long-period distributions of the nanostructure as a func-

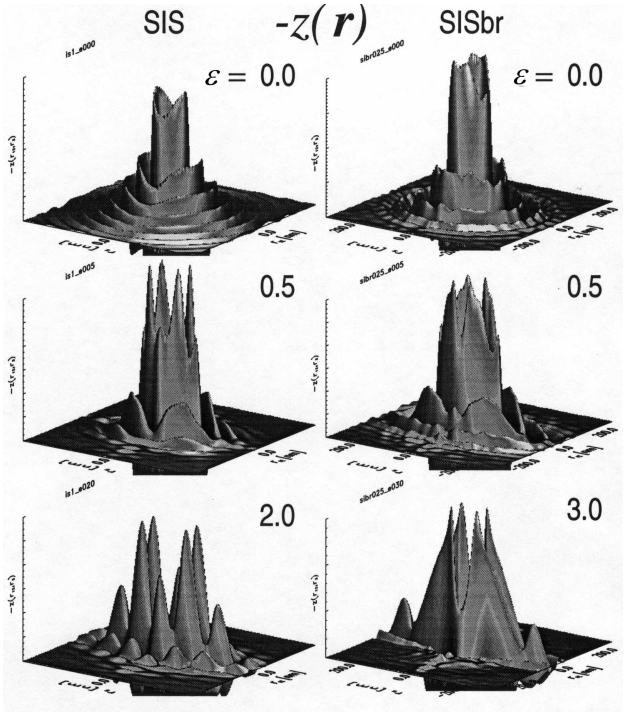

Figure 6. Three-dimensional top view ("*lattice face*") – $z(\mathbf{r})$ of the chord distribution as a function of elongation for neat (SIS) and brominated (SISbr) triblock copolymer. Peaks showing up here are long periods.

tion of elongation and position in (r_{12}, r_3)-plane. SIS at high elongation shows a well-separated arrangement of individual peaks, which is typical for any lattice. Decay of the peaks as a function of their distance from the center demonstrates loss of order (short-range order). SISbr long periods are organized differently. They are concentrated close to the meridional axis and form more or less continuous walls even at high elongation.

While for one-dimensional structures suitable model functions are at hand[33, 34] which describe and link together long-period distributions and particle size distributions, the observed variety of multidimensional peaks reveals the challenge in the task of fitting a model to the multidimensional CDF. Interpretation of these rich functions, on the other hand, may add to the understanding of nanostructure in polymer materials.

Nanostructure Extraction

After that the fundamental properties of the nanostructure have been deduced from three-dimensional plots, contour plots (Figure 7 and Figur 9) can be utilized to gain a quantitative description of the average structure from peak maxima positions in $z(\mathbf{r})$. Obviously the result is an approximation, because shape and overlap of particle correlation peaks are not considered.

Figure 7 presents CDF contour plots of the sample SIS at high elongation ($\varepsilon = 2.0$). The top plot shows the positive peaks, the bottom plot the negative peaks with labels. From the position of the strongest peaks on the meridian, (*d*), a domain height of ca. 50 nm is determined. From the width of this peak in the lateral dimension, a cylinder diameter of 8 nm is estimated. The arrangement of the polystyrene cylinders in the polybutadiene matrix can is extracted from the positions of the other observable peaks. These data result in a model of the nanostructure, which is sketched in Figure 8.

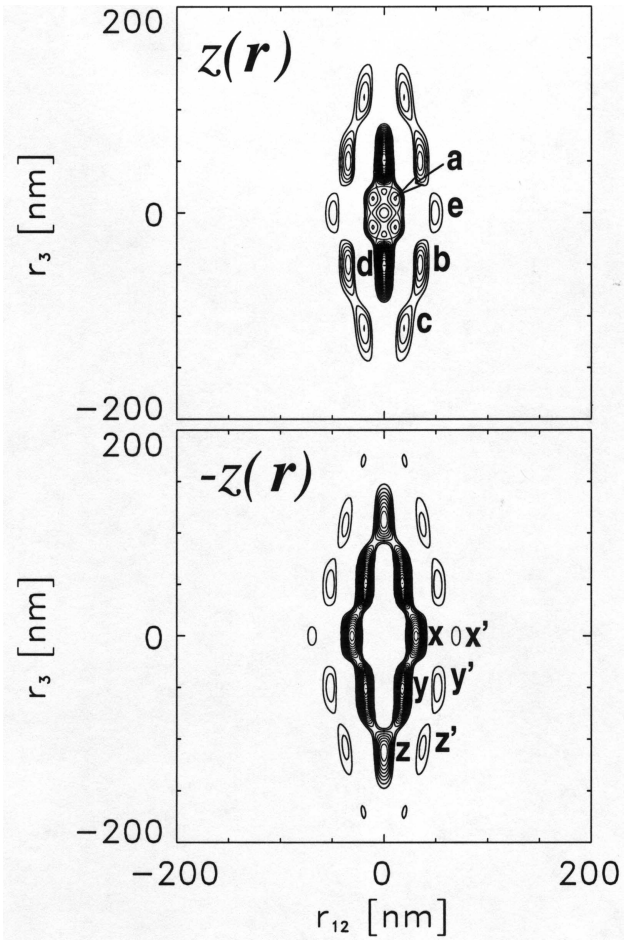

Figure 7. CDF countour plots of sample SIS at elongation $\varepsilon = 2.0$. Domain face (top) and lattice face (bottom). Peak labels correspond to labeling in a sketch of the corresponding nanostructure (Figure 8).

Peak (*a*) at a position (r_{12}, r_3) equal to (12 nm, 14 nm): reveals the displacement from a cylinder cap to the closest cap of a neighboring cylinder. (*b*), (38 nm, 50 nm): from the cylinder top cap to the bottom cap of the closest neighbor in a lateral direction. (*c*), (114 nm, 18 nm): from the top cap to the bottom cap of a cylinder displaced both in lateral and in longitudinal directions. (*d*) has already been explained. The peak from top cap to closest-neighbor top cap (*x*) is a long period. An intermitted particle is the correlation (*e*), (0 nm, 50 nm) between the left side of a cylinder and the right side of its neighbor to the right. The observed misplacement may result from asymmetric

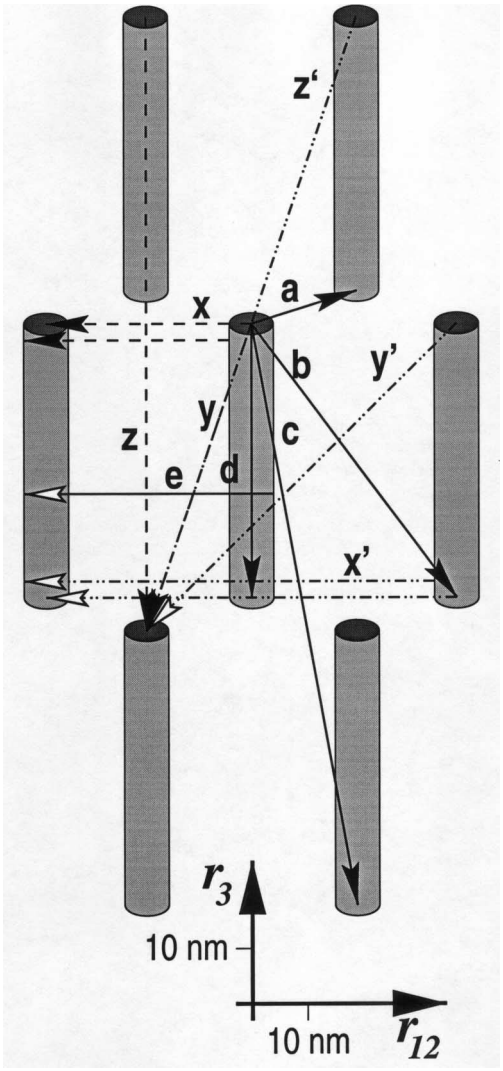

Figure 8. Nanostructure model of sample SIS at elongation $\varepsilon = 2.0$ as derived from CDF interpretation and peak position analysis (Figure 7).

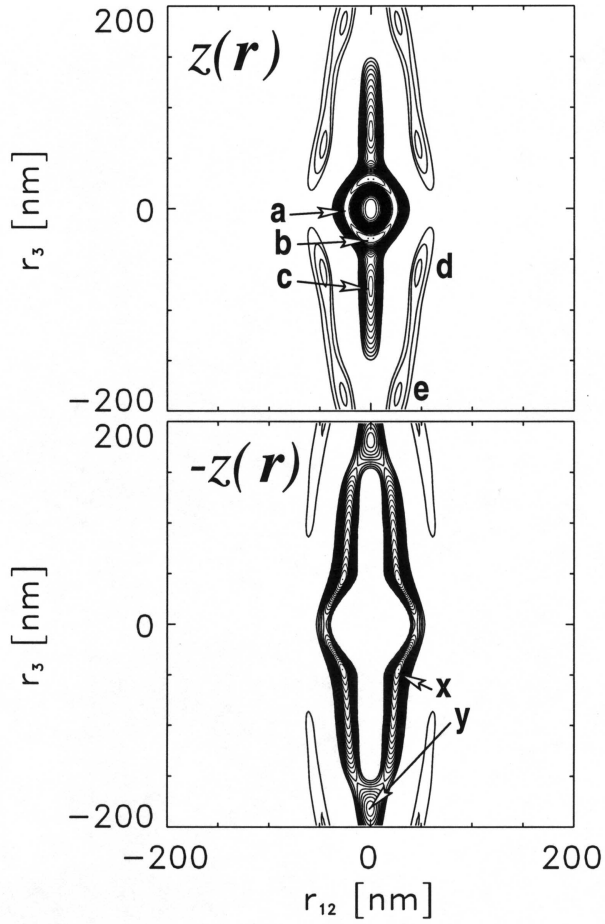

Figure 9. CDF countour plots of sample SISbr at elongation $\varepsilon = 2.0$. Domain face (top) and lattice face (bottom). Peak labels correspond to labeling in a sketch of the corresponding nanostructure (Figure 10).

shape of the particle size distributions. A different explanation would resort to a second component to the nanostructure with cylinders oriented parallel to the equator.[35, 36] The two possibilities should be distinguishable by model fit.

The closest long period in the lateral direction (x), (35 nm, 0 nm) was already mentioned. A second order in the lateral direction (x'), (70 nm, 0 nm) is seen for every long period. The other long periods are found at (y), (18 nm, 52 nm); (y'), (52 nm, 52 nm), (z), (0 nm, 114 nm), and (z'), (35 nm, 114 nm). Thus all the observed strong peaks in the CDF can be explained by a hexagonal arrangement of elongated cylinders with next-neighbor correlations only.

For the sample SISbr the corresponding set of labeled contour plots is shown in Figure 9. A model sketch is presented in Figure 10.

From the main axes of the central ellipsoidal ring an average polystyrene domain diameter of (a) = 24 nm and a height of (b) = 38 nm is determined. The ellipsoidal shape of the fundamental particle causes more pronounced peak smearing from shape than in the case of the cylinders discussed above. But moreover, the arrangement of samples inside the SISbr sample appears to be less perfect. The observed domain peaks are found at $c \approx (c_1 + c_2)/2 \approx 86$ nm; $d \approx$ (45 nm, 62 nm); $e \approx$ (27 nm, 182 nm). Here strong second orders of long periods are not observed. The highest long-period peaks are found under oblique displacement $x \approx$ (28 nm, 44 nm). The second strong long-period correlation is at the meridian $y \approx$ (0 nm, 182 nm). Everywhere on a closed path around the origin long periods are found. Only the weak second orders are found on isolated islands.

Here CDF analysis reveals that, indeed, the sample is characterized by a microfibrillar structure with correlations among particles along the meridian. Additionally the CDF shows considerable correlations among ellipsoids under oblique angle, which are not extracted by conventional SAXS analysis. Some other distinct features of the CDF, in particular the wall-shaped long periods in

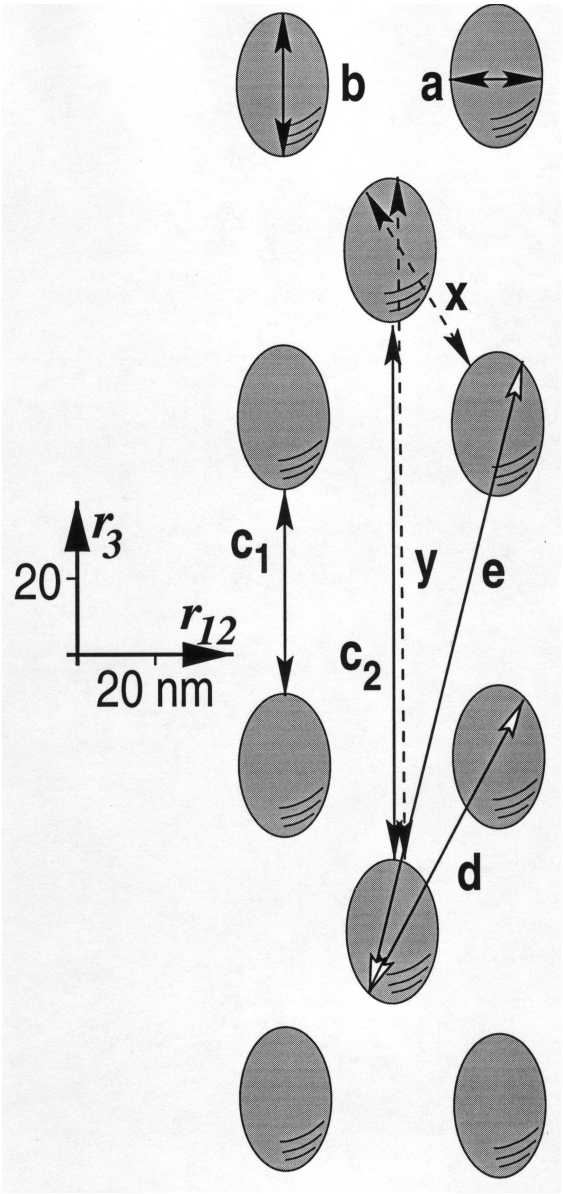

Figure 10. Nanostructure model of sample SISbr at elongation $\varepsilon = 2.0$ as derived from CDF interpretation and peak position analysis (Figure 9).

the (r_{12}, r_3)-plane, may lead to novel insight into fundamentals of such nanostructures.

Obviously, at lower elongation the basic nanostructural clusters are subject to an orientation distribution of considerable width. This fact complicates analysis of the nanostructure.

5 Conclusions

It has been demonstrated that the two-dimensional chord distribution function applied to the field of thermoplastic elastomeric materials yields information concerning the nanostructure which conforms to established fundamental notions. Moreover, structural details which are difficult to assess by other evaluation methods are clearly presented in the plots. The method appears well-suited to investigate variations of nanostructure of polymer materials on strain or temperature by time-resolved SAXS. Thus it is expected to become a valuable tool to elucidate structure forming processes as well as the relation between structure and properties of polymer materials. Based on detailed information obtained from CDF interpretation, the next challenging step will be to design model functions for CDF fitting, which additionally consider statistical variation of domain sizes and distances.

Acknowledgment: This study has been carried out in the frame of the HASYLAB project II–98–067, "Polymers with Fiber Symmetry". Support of the German and Romanian *Ministries of Education and Research* in the frame of project RUM–047–97, "Novel Block-Copolymers with Improved Service Properties" is gratefully acknowledged.

Received: August 23, 2001
Accepted: October 23, 2001

[1] G. Porod, *Kolloid-Z.* **1951**, *124*, 83.
[2] P. Debye, H. R. Anderson, H. Brumberger, *J. Appl. Phys.* **1957**, *28*, 679.
[3] C. G. Vonk, C. Kortleve, *Kolloid-Z. Z. Polymere* **1967**, *220*, 19.
[4] G. Kortleve, C. G. Vonk, *Kolloid-Z. Z. Polymere* **1968**, *225*, 124.
[5] C. G. Vonk, *J. Appl. Cryst.* **1973**, *6*, 81.
[6] C. G. Vonk, *Colloid Polym. Sci.* **1979**, *257*, 1021.
[7] G. R. Strobl, M. Schneider, *J. Polym. Sci., Part B: Polym. Phys.* **1980**, *B18*, 1343.
[8] C. Santa Cruz, N. Stribeck, H. G. Zachmann, F. J. Baltá Calleja, *Macromolecules* **1991**, *24*, 5980.
[9] J. Méring, D. Tchoubar, *J. Appl. Cryst.* **1968**, *1*, 153.
[10] D. Tchoubar, J. Méring, *J. Appl. Cryst.* **1969**, *2*, 128.
[11] J. Méring, D. Tchoubar, C. Schiller, *Bull. Soc. Fr. Mineral. Cristallogr.* **1967**, *XC*, 436.
[12] J. Méring, D. Tchoubar-Vallat, *C. R. Acad. Sci.* (*Paris*) **1965**, *261*, 3096.
[13] J. Méring, D. Tchoubar-Vallat, *C. R. Acad. Sci.* (*Paris*) **1966**, *262*, 1703.
[14] W. Ruland, *Colloid Polym. Sci.* **1977**, *256*, 417.
[15] W. Ruland, *Colloid Polym. Sci.* **1978**, *256*, 932.
[16] N. Stribeck, W. Ruland, *J. Appl. Cryst.* **1978**, *11*, 535.
[17] N. Stribeck, *Colloid Polym. Sci.* **2002**, in press.
[18] N. S. Murthy, K. Zero, D. T. Grubb, *Polymer* **1997**, *38*, 1021.
[19] N. S. Murthy, D. T. Grubb, K. Zero, *Macromolecules* **2000**, *33*, 1012.
[20] N. S. Murthy, D. T. Grubb, K. Zero, *ACS Symp. Ser.* **2000**, *739*, 24.
[21] N. Stribeck, *J. Appl. Cryst.* **2001**, *34*, 496.
[22] C. C. Honeker, E. L. Thomas, N. S. Murthy, D. T. Grubb, K. Zero, *Chem. Mater.* **1996**, *8*, 1702.
[23] M. Wohlgemuth, N. Yufa, J. Hoffman, E. L. Thomas, *Macromolecules* **2001**, *34*, 6083.

[24] D. A. Hajduk, P. E. Harper, S. M. Gruner, C. C. Honeker, G. Kim, E. L. Thomas, L. J. Fetters, *Macromolecules* **1994**, *27*, 4063.
[25] E. Buzdugan, P. Ghioca, E. G. Badea, S. Şerban, N. Stribeck, N. S. Murthy, D. T. Grubb, K. Zero, *Eur. Polym. J.* **1997**, *33*, 1713.
[26] E. Buzdugan, P. Ghioca, N. Stribeck, E. G. Badea, S. Şerban, M. C. Iovu, *Eur. Polym. J.* **1998**, *34*, 1531.
[27] D. H. Kaelble, *J. Appl. Polym. Sci.* **1965**, *9*, 1209.
[28] F. J. Baltá Calleja, C. G. Vonk, "*X-Ray Scattering of Synthetic Polymers*", Elsevier, Amsterdam 1989.
[29] A. Guinier, G. Fournet, "*Small-Angle Scattering of X-Rays*", Chapman and Hall, London 1955.
[30] O. Glatter, O. Kratky, Eds., "*Small-Angle X-Ray Scattering*", Academic Press, London 1982.
[31] L. A. Feigin, D. I. Svergun, "*Structure Analysis by Small-Angle X-Ray and Neutron Scattering*", Plenum Press, New York 1987.
[32] W. Fronk, W. Wilke, *Colloid Polym. Sci.* **1985**, *263*, 97.
[33] N. Stribeck, *Colloid Polym. Sci.* **1993**, *271*, 1007.
[34] Z. Wang, B. S. Hsiao, N. Stribeck, *Macromolecules* **2001**, in press.
[35] N. Stribeck, S. Polizzi, P. Bösecke, H. G. Zachmann, *Rev. Roum. Chim.* **1989**, *34*, 635.
[36] N. Stribeck, P. Bösecke, S. Polizzi, *Colloid Polym. Sci.* **1989**, *267*, 687.